

ELASTIC WAVE SCATTERING FROM ROUGH SURFACES AND CRACKS

S. Ayter and B.A. Auld

Edward L. Ginzton Laboratory
Stanford University
Stanford, CA 94305

INTRODUCTION

The scattering from rough surfaces and cracks in the high frequency regime is analyzed via a scattering formula based on the reciprocity relation. Scattering from the smooth cracks is investigated first to rederive the "flash point" concept by Fourier transform methods. Based on this analysis, an inversion procedure is proposed for obtaining the characteristic function of the crack, which, for the case of rough cracks, gives information about the roughness as well as the dimensions and shape of the crack. The theory is applicable to both 2-D and 3-D scattering problems, as well as surface wave scattering from surface breaking cracks. Elastodynamic ray theory predicts that scattering from cracks can be described in terms of discrete source points on the contour of the crack.¹ These points are generally called the "flash points", and their positions depend on the transmitter and receiver locations as well as the crack shape. For instance, for 2-D scattering problems, (or for deep surface breaking cracks under surface wave excitation), the two edges of the crack act as the flash points. The theoretical derivation for bulk cracks involves application of the Kirchhoff approximation for the total fields in the representation theorem, converting the surface integral into a line integral via "integration by parts," and applying the method of stationary phase to obtain the flash points.¹ In this study we use a scattering formula based on the reciprocity relation,^{2,3} with the Kirchhoff approximation and deduce the flash points by Fourier transform methods.

For the case of smooth cracks, both methods yield the same result. In the first method, because of the nature of the integrand,

the second term in the "integration by parts" step vanishes, and the first term, after some manipulations gives the flash points. However, for rough cracks, the second term no longer vanishes, and the effect of the roughness appears mainly there. Owing to the complicated nature of this second term, one cannot readily conclude about the general nature of the rough surface scattering. In our case, the method for the smooth cracks can be extended to the rough crack scattering without much difficulty, and the effects can be analyzed via simple Fourier transform relations.

SCATTERING FORMULA AND ITS APPLICATION TO SCATTERING FROM CRACKS

A scattering formula due to Auld,² and Kino³ is used to calculate the scattering coefficient. This formula has various advantages over the representation theorem. First of all, it gives the transducer-to-transducer scattering coefficient in terms of the transducer terminal voltages, which are the actual measured quantities in an experiment. Secondly, instead of the Green's function, it uses the actual transducer's far field which are essentially plane waves at the flaw. This is especially important when the Green's function is either unknown or very difficult to calculate. Thirdly, due to its relative simplicity, the mathematical steps are more tractable, and this allows more physical insight into the problem. Finally, the formulation is not restricted by the transducer types, or the excitation methods so long as the field pattern due to the excitation can be estimated.

The formula expresses the change in the scattering coefficient, $\delta\Gamma_{21}$, due to the presence of the crack as,

$$\delta\Gamma_{21} = \Gamma'_{21} - \Gamma_{21} = \frac{1}{4(P_1 P_2)^{1/2}} \oint_{S_F} (\bar{V}'_1 \cdot \bar{T}_2 - \bar{V}_2 \cdot \bar{T}'_1) \cdot \hat{n} \, dS, \quad (1)$$

where subscripts 1 and 2 indicate the particle velocity and stress field distributions excited by transducers 1 and 2 respectively, which are driven by input powers P_1 and P_2 , and the prime denotes the presence of the crack. The crack surface is designated by S_F , with the normal pointing towards the flaw being \hat{n}_F (see Fig. 1). One should note that the integral in Eq. (1) is a closed surface integral, including both faces of the crack.

For open cracks, $\bar{T}'_1 \cdot \hat{n} = 0$ on the front and back surfaces. For closed cracks, $\bar{T}'_1 \cdot \hat{n}$ is continuous across the crack. Then

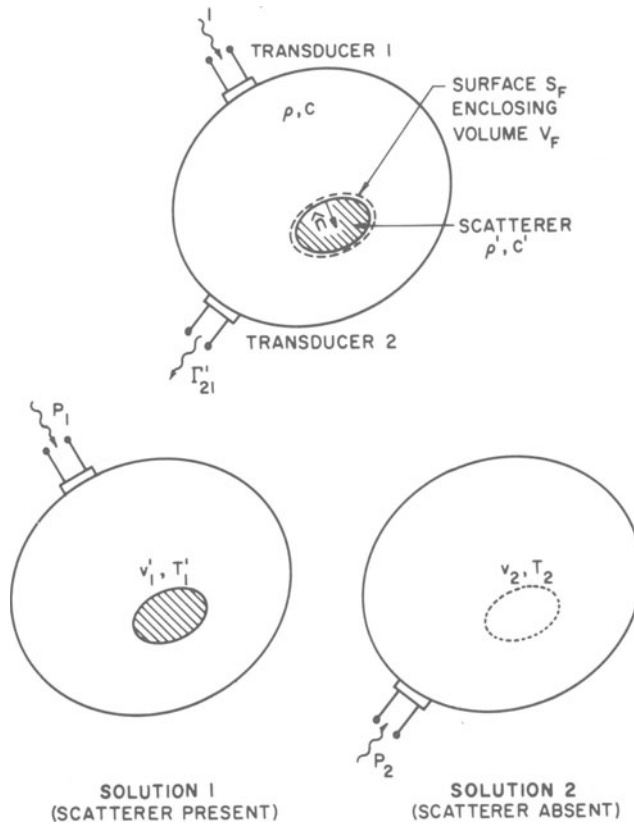


Fig. 1. Definitions of the terms used in the scattering formula.

Eq. (1) can be rewritten as

$$\delta\Gamma_{21} = \frac{1}{4(P_1 P_2)^{1/2}} \int_{\text{front face}} \Delta\bar{V}'_1 \cdot \bar{T}_2 \cdot \hat{n} \, dS \quad , \quad (2)$$

where $\Delta\bar{V}'_1$ is the jump in the particle velocity distribution across the crack.

Preliminary Considerations and Assumptions

The general scattering geometry is outlined in Fig. 2. It is assumed that the crack lies in the x-y plane and is in the far field of the transducers. Since the crack width of interest, $2c$, is in the order of several wavelengths, in the vicinity of the crack, the unperturbed fields can be approximated by plane waves, but the ampli-

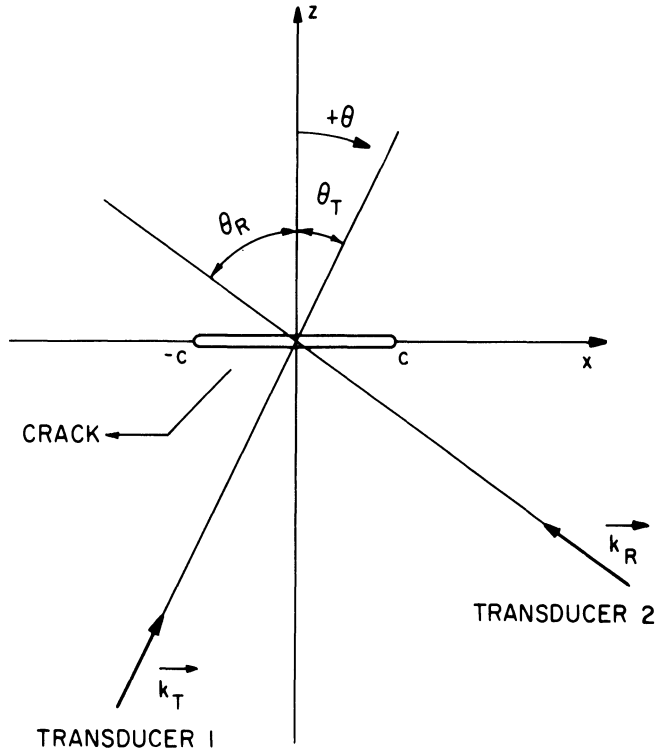


Fig. 2. General scattering geometry. In 2-D k_T and k_R are in the x-z plane, but in e-D they are not necessarily so.

tudes must be corrected for the diffraction effects. The unperturbed fields are therefore characterized by $A(\omega) \exp[j(\omega t - \hat{k}_0 \cdot \hat{k}_\alpha \cdot \vec{r})]$ where $\alpha = T$, or R corresponding to transmitter and receiver respectively, $k_0 = \omega/V$ is the wavenumber, and \hat{k}_α is the unit vector in the propagation direction. The $A(\omega)$ factor summarizes the effect of diffraction,

$$A(\omega) \sim \begin{cases} \sqrt{\omega} & \text{for } 2\text{-D} \\ \omega & \text{for } 3\text{-D} \end{cases} \quad (3)$$

In all cases, by the term scattering data, we mean the variation of the scattering coefficient in frequency, with the transmitter and receiver positions fixed. It is also assumed that in the 2-D case, the propagation vectors \hat{k}_T and \hat{k}_R are in the x-z plane, but in the 3-D case they are not necessarily so. A further assumption is that the crack location is known, i.e., the transducers are arranged so that the crack is near the center of their main lobes.

For the perturbed field distributions, we use the Kirchhoff approximation, namely, taking for the fields on the front surface those that would be present if the crack were a specular reflector, and on the back face assuming the fields to be zero. Then, for fixed transducer positions, Eq. (2) reduces to

$$\delta\Gamma_{21} \sim \int_{\substack{\text{front} \\ \text{face}}} A^2 e^{-jk_o [(\hat{k}_T + \hat{k}_R) \cdot \hat{x} x + (\hat{k}_T + \hat{k}_R) \cdot \hat{y} y]} dx dy \quad (4)$$

We next introduce $\gamma(x,y)$, the characteristic function of the crack,

$$\gamma(x,y) = \begin{cases} 1 & (x,y) \text{ on crack face;} \\ 0 & \text{elsewhere} \end{cases} \quad (5)$$

This reduces Eq. (4) to

$$\delta\Gamma_{21} \sim \int_{-\infty}^{\infty} \int_{-\infty}^{\infty} A^2 \gamma(x,y) e^{-jk_o \vec{k}_s \cdot \vec{r}} dx dy \quad (6)$$

where $\vec{k}_s = (\hat{k}_T + \hat{k}_R)$, and the direction of \vec{k}_s will be referred to as the "scan direction". Note that for back scattering ($\hat{k}_T = \hat{k}_R$), and \vec{k}_s is parallel to \hat{k}_T .

SCATTERING FROM SMOOTH CRACKS

2-D Case

For the two-dimensional case, or deep surface breaking cracks, the characteristic function is a function only of x . Using Eq. (3), the counterpart of Eq. (6) for the 2-D case is found to be

$$\delta\Gamma_{21}(\omega) \sim \omega \int_{-\infty}^{\infty} \gamma(x) e^{-jk_o \vec{k}_s \cdot \hat{x} x} dx \quad (7)$$

From $k_o = \omega/V$ and the definition

$$\tau = \vec{k}_s \cdot \hat{x} \left(\frac{x}{V} \right) \quad (8)$$

where V is the phase velocity of the wave of illumination, one readily sees that

$$\delta\Gamma_{21}(\omega) \sim \omega \mathcal{F}\{\bar{\gamma}(\tau)\} \quad (9)$$

where

$$\bar{\gamma}(\tau) = \gamma\left(\frac{V\tau}{\vec{k}_s \cdot \hat{x}}\right) \quad (10)$$

and $\mathcal{F}\{\cdot\}$ is the Fourier transform operation from the τ domain into the ω domain. Using the time differentiation property of Fourier transformation,⁴ Eq. (9) can be expressed as,

$$\delta\Gamma_{21}(\omega) \sim \mathcal{F}\left\{\frac{d}{d\tau}\bar{\gamma}(\tau)\right\} \quad (11)$$

Equation (11) states that $(d/d\tau)\bar{\gamma}(\tau)$ and $\delta\Gamma_{21}(\omega)$ are Fourier transform pairs. Therefore, in the time domain with pulse operation two pulses of opposite phase are observed at the receiving transducer, with a time difference (see Fig. 3)

$$\Delta\tau = 2c \vec{k}_s \cdot \hat{x} / V \quad (12)$$

corresponding to the time delay between the rays that hit the edges of the crack and return to the receiver. Therefore, the signal appears as if it is coming from the edges (flash points). Figure 3 schematically illustrates the argument.

3-D Case

For the three-dimensional case, Eq. (6) can be interpreted in terms of the two-dimensional Fourier transform of the characteristic function $\gamma(x,y)$ from the x - y domain into the k_x, k_y domain, where

$$\begin{aligned} k_x &= \frac{\omega}{V} (\vec{k}_s \cdot \hat{x}) \quad , \quad \text{and} \\ k_y &= \frac{\omega}{V} (\vec{k}_s \cdot \hat{y}) \quad . \end{aligned} \quad (13)$$

Since the transducer positions are fixed, the components of the projection of the scan vector \vec{k} on the crack plane, $\vec{k}_s \cdot \hat{x}$ and $\vec{k}_s \cdot \hat{y}$ are fixed quantities.⁵ Therefore, as the frequency changes, the scattering coefficient scans the Fourier domain along the line

$$k_y = \frac{\vec{k}_s \cdot \hat{y}}{\vec{k}_s \cdot \hat{x}} k_x \quad (14)$$

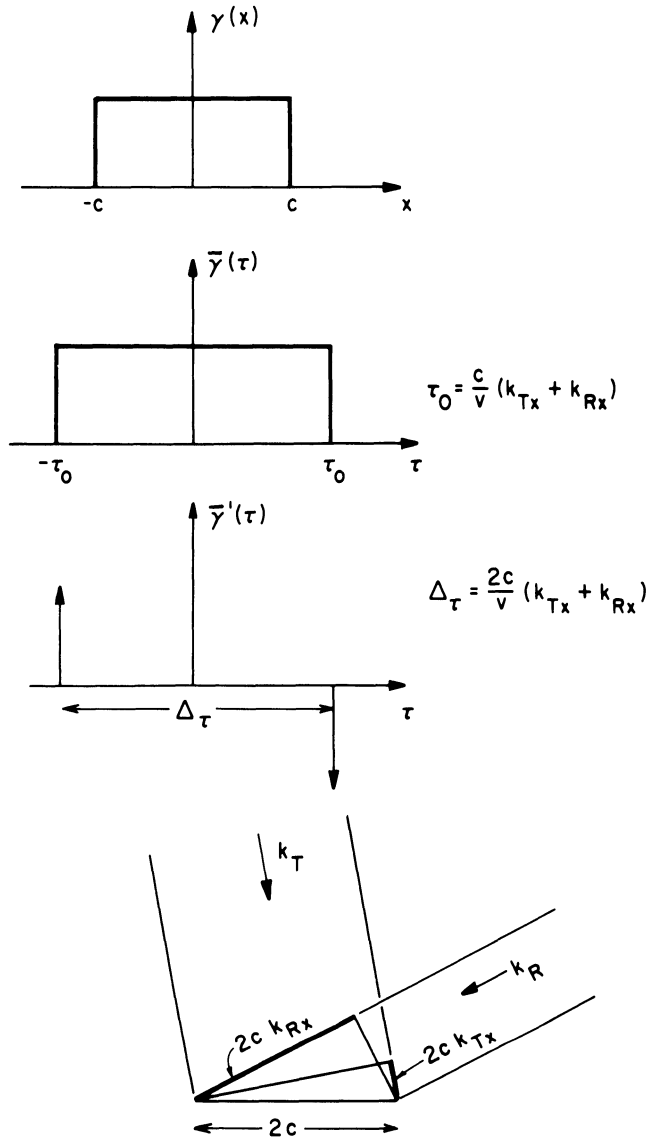


Fig. 3. Scattering mechanism for the 2-D case. The same argument applies to the Rayleigh wave scattering from deep surface breaking cracks.

Rotating the coordinates in the x-y plane via the coordinate transformation

$$\begin{aligned}
 \tau &= [(\vec{k}_s \cdot \hat{x})x + (\vec{k}_s \cdot \hat{y})y]/V \quad , \\
 \upsilon &= [-(\vec{k}_s \cdot \hat{y}) + (\vec{k}_s \cdot \hat{x})y]/V \quad ,
 \end{aligned}
 \tag{15}$$

one can rewrite Eq. (6) as,

$$\delta\Gamma_{21}(\omega) \sim \omega^2 \int_{-\infty}^{\infty} \left[\int_{-\infty}^{\infty} \underline{\gamma}(\tau, \nu) d\nu \right] e^{-j\omega\tau} d\tau \quad , \quad (16)$$

where

$$\underline{\gamma}(\tau, \nu) = \gamma \left(\frac{V}{|k_s|^2} (\vec{k}_s \cdot \hat{x} \tau - \vec{k}_s \cdot \hat{y} \nu) \quad , \quad \frac{V}{|k_s|^2} (\vec{k}_s \cdot \hat{y} \tau + k_s \cdot \hat{x} \nu) \right) \quad . \quad (17)$$

Defining $\bar{\gamma}(\tau)$ as the integral of $\underline{\gamma}(\tau, \nu)$ along the direction normal to the scan direction, i.e.,

$$\bar{\gamma}(\tau) = \int_{-\infty}^{\infty} \underline{\gamma}(\tau, \nu) d\nu \quad , \quad (18)$$

one can interpret Eq. (16) as

$$\delta\Gamma_{21}(\omega) \sim \mathcal{F} \left\{ \frac{d^2}{d\tau^2} \bar{\gamma}(\tau) \right\} \quad . \quad (19)$$

The procedure is outlined schematically in Fig. 4. The limits of $\bar{\gamma}(\tau)$ are defined at the points where the tangent line to the contour of $\underline{\gamma}(\tau, \nu)$ is in the ν direction, and the slope of $\bar{\gamma}(\tau)$ is discontinuous at those points. As a result, the second derivative shows a corresponding impulsive behavior. As in the 2-D case, these are the flash points time domain because of Eq. (19).

INVERSION SCHEME

The flash points are basically the result of the diffraction mechanism. Therefore if one takes the effect of diffraction from the scattering data, one can obtain directly the characteristic function of the crack. In mathematical form,

$$\bar{\gamma}(\tau) = \begin{cases} \mathcal{F}^{-1} \{ \delta\Gamma(\omega)/\omega \} & \text{2-D case} \quad , \\ \mathcal{F}^{-1} \{ \delta\Gamma(\omega)/\omega^2 \} & \text{3-D case} \quad . \end{cases} \quad (20)$$

This inversion procedure gives the crack dimensions, as well as the information about the crack shape for the 3-D case. For instance, with a single measurement it is possible to determine both dimensions of the crack, provided that the crack orientation is known (see Fig. 4).

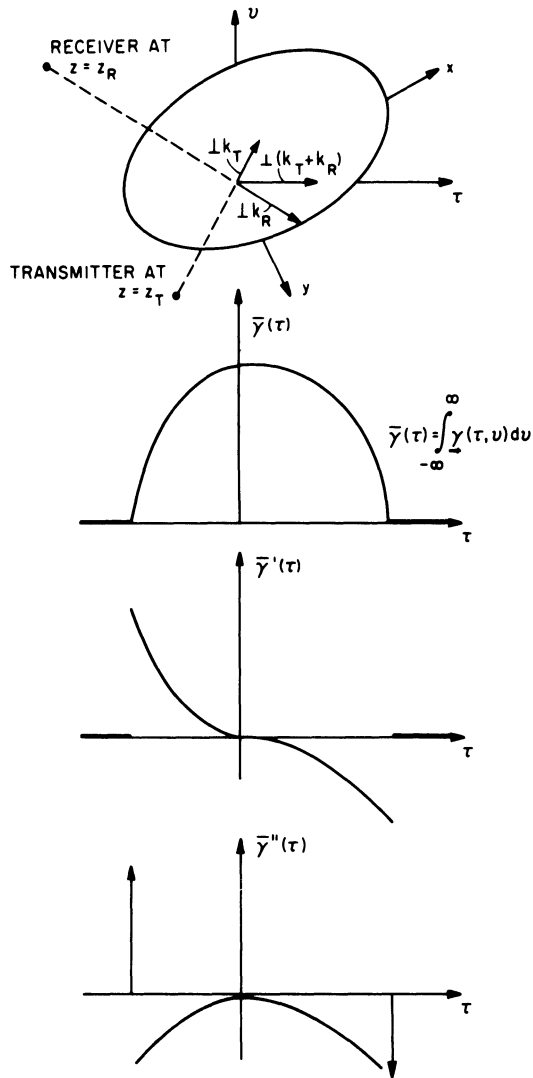


Fig. 4. Scattering mechanism for the 3-D case.

The weakness of the procedure lies in the fact that the Fourier inversion mechanism requires the data over the whole ω -domain. When the data is bandlimited, sharp variations in the actual characteristic function will cause oscillations in the inverted data (Gibbs phenomenon).⁴ However, this problem is equipment related, and with wider band transducers its effect can be reduced.

The inherent problem of the inversion method is that it is valid only in the high frequency regime. Therefore, even if the transducer can excite low frequencies efficiently, the data at low frequencies

may not agree with the theoretical expectations, hence one may have to reject that data, or analyze it via low frequency theories.

ROUGH CRACKS

Relevance to Fracture Mechanics

As a crack grows under cyclic loading, it exhibits different roughness characteristics in different growth regimes. A typical plot of growth rate vs effective stress intensity is shown in Fig. 5. In Regime I, the crack growth is via non-continuum mechanisms, and mainly affected by the microstructure. For this reason, face roughening is the dominant character. In Regime II, the microstructure has little influence on crack growth and the crack propagates in continuum. In this regime, the crack tip is continuously blunted and reshaped. Therefore, although the crack faces are smoother, the crack tip grows irregularly.⁵

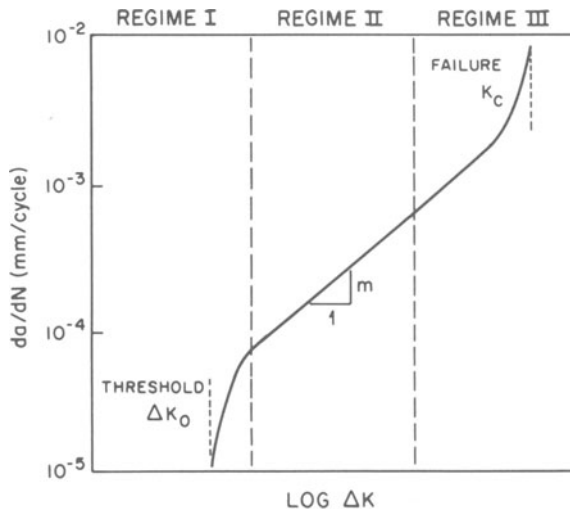


Fig. 5. Crack growth rate, da/dN , as a function of the stress intensity range, ΔK .

been found that⁸ the contribution of the rough surface alone, $(\delta\Gamma)_r$ will be proportional to

$$(\delta\Gamma)_r \sim -jk_o(k_T + k_R)_z \zeta(x,y) \quad (21)$$

where $\zeta(x,y)$ is the roughness function.

The second method considered is an extension of Kirchhoff boundary conditions to the rough surfaces, described in the literature as "the tangent plane approximation".⁹ In this case one takes the total field as the sum of incident wave plus the specularly reflected waves from the local tangent plane to the rough surface. When the transducer angles are around normal incidence with respect to the rough surface, mode coupling is negligible provided that the roughness amplitude is less than ~ 0.2 wavelengths. The results of scalar diffraction theory will then apply and one finds,

$$\begin{aligned} \delta\Gamma &\sim \delta\Gamma^{(o)} e^{-jk_o(k_T+k_R)_z \zeta(x,y)} \\ &\approx \delta\Gamma^{(o)} [1 - jk_o(k_T + k_R)_z \zeta(x,y) + \dots] \quad , \end{aligned} \quad (22)$$

in agreement with the results of perturbation analysis.

The perturbation analysis is valid for roughness amplitudes $|\zeta(x,y)|_{\max} \ll 1$ and for its slope

$$\left| \frac{\partial}{\partial \alpha} \zeta(x,y) \right|_{\max}^2 \ll 1 \quad , \quad \alpha = x,y .$$

The tangent plane method is also valid for small variations in slopes, but can tolerate larger roughness amplitudes. Another approach being considered is to model the roughness as a superposition of small, known geometry, scatterers with a random distribution. In this case, each scatterer is small compared to the wavelength, hence the field disturbances around each scatterer can be visualized via quasi-static field theory. This kind of model permits faster variations for the roughness function since the disturbance due to each scatterer is tightly localized, and the adjacent scatterers do not interact to first order. With this kind of model, the result is also the same as that given by Eq. (22).

With the above models for an open crack, the characteristic function for a rough crack can be seen to be of the form

$$\begin{aligned} \gamma_r &= \gamma(x,y) e^{-jk_o \vec{k}_s \cdot \hat{z} \zeta(x,y)} \\ &\approx \gamma(x,y) [1 - jk_o \vec{k}_s \cdot \hat{z} \zeta(x,y) + \dots] \quad . \end{aligned}$$

If the crack is closed at certain spots, the characteristic function will show a jump at the closure point. For instance, if the faces contact rigidly, i.e., $\Delta \bar{V}'_1 = 0$, then $\gamma_r = 0$ at those points.

INVERSION OF ROUGH CRACKS

Unlike the smooth crack case, the characteristic function of rough cracks is frequency dependent, and in general the Fourier inversion algorithm does not apply. However when $\vec{k}_s \cdot \hat{z} \zeta(x,y) \ll 1$, the characteristic function can be approximated as,

$$\gamma_r(x,y,\omega) \approx \gamma(x,y) - j\omega\gamma(x,y) \frac{\vec{k}_s \cdot \hat{z}}{V} \zeta(x,y) / V .$$

The inversion algorithm then gives the sum of the smooth crack characteristic function, and the roughness contribution, which is proportional to the derivative of the roughness function, i.e.,

$$\mathcal{F}^{-1}\{\delta\Gamma_{21}(\omega)/\omega\} = \bar{\gamma}(\tau) \left[1 + \frac{\vec{k}_s \cdot \hat{z}}{V} \frac{d}{d\tau} \zeta(\tau) \right]$$

for the 2-D case, and

$$\mathcal{F}^{-1}\{\delta\Gamma_{21}(\omega)/\omega^2\} = \bar{\gamma}(\tau) \left[1 + \frac{\vec{k}_s \cdot \hat{z}}{V} \frac{d}{d\tau} \int_{-\infty}^{\infty} \zeta(\tau,\nu) d\nu \right]$$

for the 3-D case. Hence, for the 3-D case one measures the roughness function in the scan direction.

In the flash point representation of scattering from a rough crack, the second (2-D case) and third (3-D case) derivatives of the roughness function are superimposed on the regular flash points. Hence, any sharp variations in the roughness function will appear as secondary flash points in the scattering data.

REFERENCES

1. J.D. Achenbach, K. Wiswanathan, and A. Norris, "An Inversion Integral for Crack-Scattering Data," Wave Motion, 1:299 (1979).
2. B.A. Auld,, "General Electromechanical Reciprocity Relations Applied to the Calculation of Elastic Wave Scattering Coefficient," Wave Motion, 1:3 (1979).
3. G.S. Kino, "The Application of Reciprocity Theory to the Scattering of Acoustic Waves by Flaws," J. Appl. Phys. 49:3190 (1978).

4. A. Papoulis, "The Fourier Integral and its Applications," McGraw Hill, New York (1962).
5. R.O. Ritchie, S. Suresh, D.M. Parks, E.K. Tschegg, and S.E. Stanzl, Research on Fatigue Thresholds, in: "Fatigue Thresholds," Proceedings of the International Symposium, Stockholm, June 1981, J. Bäcklund, A.F. Blom, and C.J. Beevers, eds., EMAS Publ. Ltd., Warley, U.K. (1981).
6. M.L. Kachanov, "A Microcrack Model of Rock Inelasticity, Part II: Propagation of Microcracks," Mechanics of Materials, 1:29 (1982).
7. L.M. Brekhovskikh, "Propagation of Surface Rayleigh Waves along the Uneven Boundary of an Elastic Body," Sov. Phys.-Acous. 5:288 (1959)
8. S. Ayter and B.A. Auld, "Resonances and Crack Roughness Effects in Surface Breaking Cracks," Proceedings of DARPA/AFWAL Review of Progress in Quantitative NDE, La Jolla, July 1980, 348-354 (1981).
9. P. Beckman and A. Spizzichino, "The Scattering of Electromagnetic Waves from Rough Surfaces," Pergamon Press (1963).

ACKNOWLEDGEMENT

This work was sponsored by the Center for Advanced Nondestructive Evaluation, operated by the Ames Laboratory, USDOE, for the Air Force Wright Aeronautical Laboratories/Materials Laboratory and the Defense Advanced Research Projects Agency under Contract No. W-7405-ENG-82 with Iowa State University.